Relationships between deformation and microstructure evolution and minimizing surface roughness after BCP processing in RRR Nb cavitites

ILC-Americas University-based Accelerator R&D Progress Report

T.R. Bieler, D. Baars, K.T. Hartwig, C. Compton, T.L. Grimm

Project Overview

Three strategies for improving the surface finish of niobium sheet used in cavities were identified in the funded proposal,

1) Examine how process variables such as crystal orientation and welding affect the "single crystal" material (may be a cost effective alternative to rolled material).
2) Identify effects of rolling variables on surface texture, dislocation density, and recrystallization, to identify optimal conventional rolling approaches.
3) Further reduce the grain size and improve rolling uniformity using equal channel angle extrusion (ECAE) to pre-condition billets before rolling, and evaluate effects on heterogeneity in the microstructure and etching characteristics.

With the budget allocated, we decided to focus on items 1 and 3, which taken together will inform the issues related to item 2, and hence obtain the best impact for the resources provided. Thus, the following will review progress on deformed and recrystallized single crystal specimens, and on the effects of ECAE pre-processing of Nb on microstructure and texture. An overview of this work to date has been developed as a paper that is in press for *JOM*, to be published in June 2007; highlights from this work are provided below. The report will close with the test plan for the single crystal specimens that will be examined in the coming year.

Initial Material: The starting condition for making any RRR niobium products are the ingots that contain very large crystals (30-300 mm grain dimensions in a ~300 mm diameter ingot). Slices from the ingots used to make make prototype single or multi-crystal cavities also provided samples to examine deformation and recrystallization effects. For ECAE processing, 25 mm square x 150 mm long billets containing not more than a few crystal orientations were used.

Analysis of many conventionally rolled and recrystallized specimens show heterogeneous texture gradients that are never alike. This implies that the deformation characteristics depend on the initial crystal orientations in the starting billet, and hence, every batch of sheet niobium has a different deformation and recrystallization history. Thus the two approaches, 1) of avoiding rolling altogether in the single/multi-crystal approach, and 3) deforming the Nb so severely that the prior crystal orientation effects are obliterated, provide dramatically contrasting approaches that allow fundamental physical understanding of relationships between niobium forming and surface quality to be identified.

ECAE pre-processing of ingots

This work was conducted in collaboration with K.T. Hartwig, of Shear Form Inc. which has extended work done in a DOE funded phase I SBIR project. Equal Channel Angular Extrusion (ECAE) provides a means to homogenize the microstructure, and engineer a favorable texture before rolling into sheet. ECAE generates uniform severe plastic deformation during each pass (~200% strain for an idealized 90° angle, assuming simple shear). As the billet cross section does not change during extrusion, one may rotate the billet about its long axis between repeated passes, generating shear on different planes in the sample coordinate system, as illustrated in Figure 1 [1]. Thus ECAE enables more opportunities for applying strain in different directions than conventional rolling, providing an ability to control the deformation history to intentionally obtain textures different from those produced by conventional rolling.

Beginning with a coarse-grained ingot (like those used for commercially rolled Nb), 25 x 25 x 150 mm bars consisting of 1-5 large grains each were processed with several different processing routes at Shear Form Inc. After ECAE processing, the bars were rolled from 25mm to 4mm thick sheet. Recrystallization annealing was done at 900°C for 90 min in a vacuum. A pair of OIM scans approximately 1.5mm apart, and extending about two-thirds into the thickness from either surface of the

sheet, were taken for each of 6 specimens with different processing histories. The OIM scan provides grain size information shown in Figure 2, and the texture/microstructure of two of these 6 are shown in Figure 3. The recrystallized grain size varied somewhat due to the different deformation histories, but the average grain size for all deformation histories was 18±3μm, as illustrated in Figure 2, about half of the grain size achieved in commercially rolled material. While the average grain size was similar for both samples, the textures were completely different. For example, sample F1 had weak <001> || sheet normal direction (ND) and strong <111> || ND texture components, whereas sample L1 had modest <001> || ND and weak <111> || ND components (Figure 3), and it had greater variance in the average grain size between the two scans (Fig. 2). Though the grain size appears fairly uniform and small (much more uniform than conventionally rolled material), there is still microstructural heterogeneity present that is evident in the form of texture gradients (color gradients in the figure) and some significantly larger grains.

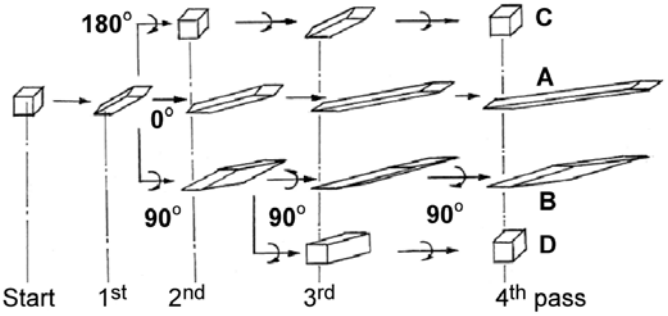

Figure 1 Simple shear history of an initial cubic element due to different ECAE deformation histories [1]

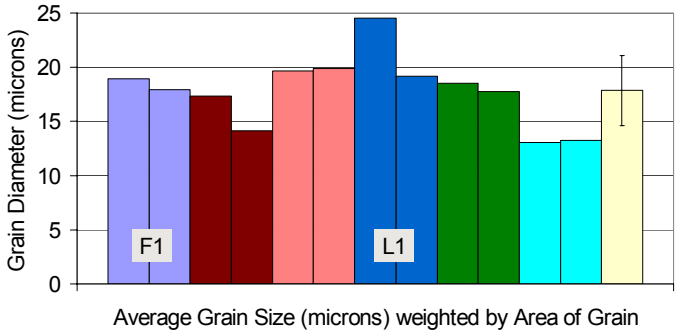

Figure 2 Average grain sizes of different ECAE processed sheets. Column at far right with error bar shows mean and standard deviation of 12 measurements of specimens with 6 deformation histories.

Sample F1 has one strongly preferred orientation on the γ fiber. Highly preferred crystal orientations on the γ fiber are known to promote excellent formability in BCC metals; this set of orientations would result in a distribution of crystal orientations that populate the entire (red) ring in the 111 pole figure in Figure 3. However, the three peaks in the (001) and four peaks in the (111) pole figures imply only a single predominant crystal orientation, that is a likely indicator of anisotropic properties in the sheet plane, despite this orientation being on the γ fiber. There was not enough material to examine the anisotropy of this specimen, so making more material with this or similar processing history is a desirable next step, to evaluate the viability of this process path.

Clearly, the recrystallized texture of rolled + annealed samples depended heavily on the cold-worked texture, which had different preferred crystal orientations. Recently, Sandim et al. [2,3] identified deformation banding in coarse-grained niobium as a mechanism that stimulated grain refinement during recrystallization, but banding depended strongly on the grain orientation. The geometrically necessary dislocations which surround deformation bands within a grain have stored strain energy, and serve as nucleation sites for recrystallization. The influence of crystal orientation on recrystallization is considered next in experiments that examine the single crystal strategic approach to making cavities.

Welding of Deformed Single Crystals

Because microstructures are inherently variable in rolled and recrystallized sheet, bypassing rolling entirely by slicing sheets from large multi-crystal ingots may be an effective strategy for making cavities. Though each of the grain orientations deform differently in biaxial drawing, leading to significant differential thinning, cavities made from these large grain slices have performed comparably with the best cavities made from polycrystals [4]. However, such deep drawn cavity halves must still be welded together. Because the welds occur in regions where the greatest strains develop during forming (and the highest electric and magnetic fields develop at these weld locations in operation), it is important

to assess how much strain can be tolerated before generating recrystallization that may adversely affect the benefits that come from single crystals.

A deformed single crystal tensile specimen was subjected to heating similar to a weld on one end to determine if recrystallization occurred, in the specimen shown at the bottom of Figure 4. From the reduction of area, the local strain at the neck was ~65%. The orientation of the deformed crystal was determined using OIM, and subsequently heated at the end closer to the neck with a TIG welding electrode to approximate a welding operation at the location noted in Figure 4 (it was heated so that the neck was kept yellow-white hot for about 20 s, but the surface did not melt). The orientations were compared before and after the weld in the same locations identified as a, b, c (c is the same location as a, but after the weld), indicating that indeed recrystallization occurred.

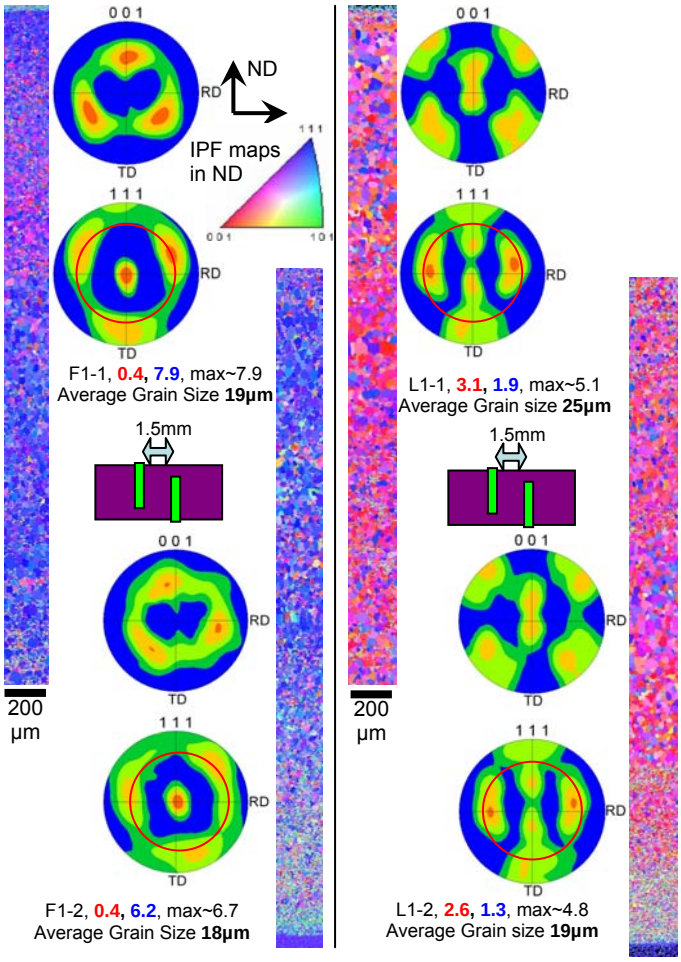

Figure 3. Microstructure and texture comparison between ECAE processed + rolled and annealed samples F1 (left side) and L1 (right side). Numbers below pole figures represent component with <100> (red) and <111> (blue) || ND.

Prior recrystallization studies in rolled sheet by Jiang et al. [5] showed that recrystallization did ***not*** occur like IF (interstitial-free) steel [6-8]. Iron differs from Nb in having a transformation that generates very fine carbides, but like pure Nb, it has a low interstitial content. The recrystallized texture of Nb was much weaker, suggesting that there are no strongly preferred recrystallization orientations in Nb. One of the possible reasons for this difference is that the elastic anisotropy of Nb and Fe are opposite of each other, as shown in Figure 5 [9,10]. The contribution of elastic modulus to recrystallization has been identified by Lee as having a strong impact on recrystallized grain growth in many materials [11,12], which is typically not considered in other studies of recrystallization in Fe [6-8]. Lee's maximum strain energy release model predicts that a recrystallized grain will lower elastic strain energy most by aligning a crystallographic minimum stiffness (E, Young's modulus) direction with the absolute maximum internal stress direction. The maximum internal stress direction is found from the cold-worked state, and taken to be the slip direction, if only one slip system is dominant, or the vector sum of the slip directions if more than one is highly active [12]. This implies that recrystallization depends not only on plastic but elastic properties as well.

The maximum internal stress direction was calculated according to Lee's model, assuming that any of the 48 slip systems in BCC with a Schmid factor of 0.4 or greater would be active and that all contributed equally to slip. The maximum internal stress direction is illustrated (projected red arrow) on the orientation maps in Figure 4. The deformed crystal modulus along this direction was determined to be 90 GPa, a fairly compliant direction (Nb is most compliant in <111> (~83 GPa) and stiffest in <100> (~145 GPa)). Very near the heat source in a region with only ~9% strain, Figure 4b, the stiffness values of the two observed recrystallized grains were higher, but the smaller grain with the higher stiffness along the original maximum strain energy direction was choked out by a lower modulus grain; the heat flow direction was from left to right. Approximately 10mm from the heat source near the furthest extent of

observed recrystallization, where the strains were larger, the largest grains did have slightly lower stiffness values, in agreement with the model. Notably, the smaller grains with higher stiffness values along the top are actually on the edge of the sample, and they clearly did not grow preferentially. At the neck, where the largest strains were located, no recrystallization was observed, perhaps due to the low temperature and short time from the passing weld. This dramatic recrystallization clearly shows that details of deformation and thermal history can lead to significant variations in recrystallization.

Lee's theory does predict the decrease in stiffness values observed in the largest grains, and the high stiffness grains tend to be small. The apparent violations occur when the maximum internal stress direction already coincides with a compliant direction. Slip in BCC occurs on {110}<111>, followed by {112}<111> and {123}<111>. This implies that dislocation pileups will occur along <111> directions with increasing strain, but because this is also the most compliant crystal direction, the elastic strain energy based advantage for a neighboring grain to consume such a high dislocation density grain will be low. This effectively undercuts the minimization of elastic strain energy that is the driving force for this model. Thus, the details of recrystallization should then depend more strongly on other criteria, such as oriented growth models that depend on substructure development [6-8]. Nevertheless, Lee's model helps account for the fact that recrystallization textures are not as well defined as in many other BCC metals, and it clearly shows that recrystallization models that consider details of dislocation substructure as well as elastic strain energy are needed to predict recrystallization in high purity Nb.

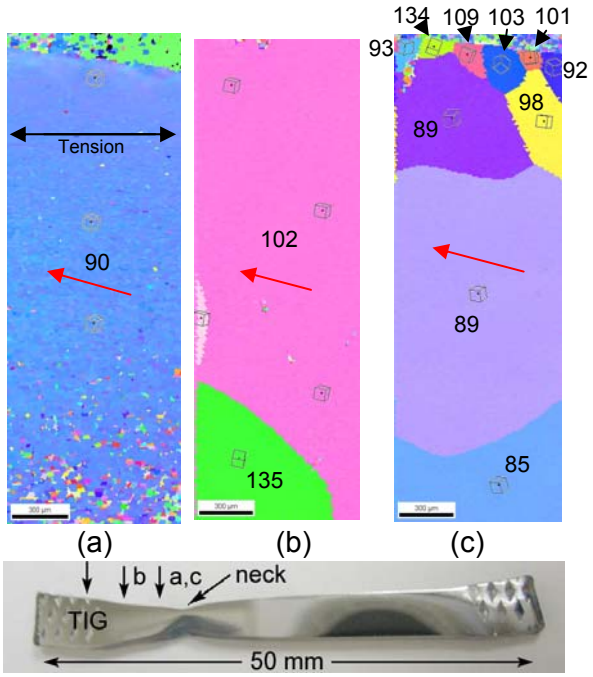

Figure 4. OIM maps (with respect to normal direction) of initially single crystal Nb deformed in tension to ε~65% near the neck; a) ~10mm to the right of the TIG heat source prior to heating, b) after heating, in an area near the heat source that was deformed to ε~9%, and c), same area as a) after heating. Numerical values are Young's Modulus in GPa of the crystal orientation along the maximum internal stress direction in deformed specimen (indicated by red arrows). Regions of speckled colors in (a) are artifacts of incomplete oxide removal during polishing.

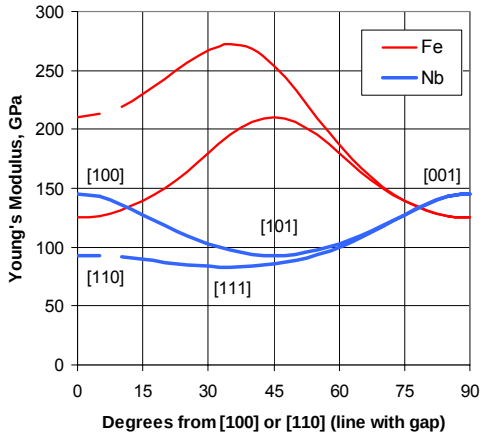

Figure 5. Crystallographic elastic anisotropy in Nb and Fe [9,10]

Project Activities and Deliverables in Coming Year

These results indicate both promise, and that difficulties need to be overcome to optimize either of the processing strategies to make higher performance cavities. The experiments described above are from initial studies, and a more focused experimental plan for a systematic study on a group of specimens that incorporate assessment of process effects on surface finish in the context of steps to make cavities is outlined below (steps 1,2 are nearly completed, and steps 3-5 are in preparation at the time of writing):

1. The outer rims from multi-crystal sheets have been prepared for tensile experiments similar to Figure 5. These specimens have been polished mechanically, electropolished sufficiently to conduct OIM investigations to obtain crystal and boundary orientation measurements.
2. Predict which slip systems will be most active from Schmid factor analysis

3. Use electron channeling contrast imaging (ECCI) to characterize initial dislocation density
4. Measure surface roughness
5. XPS on selected specimens to identify oxygen profile with depth
6. Mask some areas and conduct BCP etch, measure surface roughness on known grain orientation,
7. Mark back side with grid to provide means for differential image correlation to measure local strains, and deform in tension to desired strain of ~40% (similar to strains in iris region of cavity)
8. Measure surface roughness (at and near GB and in grain interior regions)
9. Conduct OIM/ECCI to measure grain rotations, and dislocation characteristics (repolish)
10. BCP etch, measure surface roughness on deformed surface
11. On selected specimens, XPS in vacuo + vacuum heating to evaluate effect of O diffusion depth with respect to crystal orientation/grain boundaries
12. Use recrystallization models to estimate (hypothesize) likely recrystallization orientations
13. Instrument specimens with several thermocouples, and conduct strategic EB or TIG welding runs between regions of specimens with known strains and crystal (mis)orientations
14. XPS to determine oxide character near weld
15. Electropolish as needed to gain suitable surface for OIM/ECCI evaluation of recrystallization
16. Analyze with respect to recrystallization models, develop model and criteria for predicting Rx

After step 11, on selected specimens, a purification vacuum anneal prior to welding (e.g. with Ti getter layer + etch), will be followed by XPS to assess oxide character, repolishing + surface roughness and OIM/ECCI to assess microstructure changes, and then return to step 12. With this process completed on a number of specimens with different grain orientations, the relationships between grain orientation, recrystallization, oxidation and surface finish can be identified systematically.

References:

1. Segal VM, Engineering and commercialization of equal channel angular extrusion (ECAE), Materials Science and Engineering A386, 269-76, 2004.
2. Sandim HRZ, Lins JFC, Pinto AL, Padilha AF. Recrystallization behavior of a cold-rolled niobium bicrystal. *Mat. Sci. Eng.*, A354, 217-228, Elsevier 2003.
3. Sandim, HRZ; Raabe, D, EBSD study of grain subdivision of a Goss grain in coarse-grained cold-rolled niobium, Scripta Materialia, 53 (2) 207-212 2005.
4. Kneisel, P, Myneni, GR, Ciovati, Sekutowicz, GJ, Carneiro, T, Preliminary Results From Single Crystal and Very Large Crystal Niobium Cavities, in Proceedings of the 2005 Particle Accelerator Conference, p. 3991-3993, 2005.
5. Jiang, H, Bieler, TR, Compton, C, Grimm, TL, Cold Rolling Evolution in High Purity Niobium Using a Tapered Wedge Specimen (12th International workshop on RF Superconductivity (SRF 2005)), Physica C 441 (2006), pp. 118-21.
6. Barnett MR, Kestens L, Formation of {111}< 110 > and {111}< 112 > textures in cold rolled and annealed IF sheet steel , ISIJ International 39(9), 923-929 1999
7. Choi SH, Cho JH, Primary recrystallization modelling for interstitial free steels, Materials Science and Engineering A 405 (1-2), 86-101, 2005.
8. Park YB, Lee DN, Gottstein G, Evolution of recrystallization textures from cold rolling textures in interstitial free steel, Materials Science and Technology 13 (4), 289-298 1997.
9. Armstrong, PE, Dickinson, JM and Brown, HL, Temperature dependence of the elastic coefficients of niobium (columbium) Trans. Metal. Soc. AIME 236, 1404-8, 1966.
10. Hearmon, RFS, The elastic constants of anisotropic materials, Rev. Mod. Phys, 18, 409-440, 1946.
11. Park YB, Lee DN, Gottstein G, Evolution of recrystallization textures from cold rolling textures in interstitial free steel, Materials Science and Technology 13 (4), 289-298 1997.
12. Lee DN, Relationship between deformation and recrystallization textures of fcc and bcc metals, Philosophical Magazine 85 (2-3), 297-322, 2005.